

**INFLUENCE OF TOPOGRAPHY ON SURFACE RADIO REFRACTIVITY PATTERNS  
OVER NORTH CENTRAL, NIGERIA**

**AJILEYE, O. O<sup>1</sup>, KOLAWOLE, I. S<sup>1</sup>, OGBOLE, J. O<sup>1</sup>, ALAGA, A. T<sup>1</sup>,**

**HALILU, A. S<sup>2</sup> and MOHAMMED, S. O<sup>2</sup>**

**Abstract**

This paper investigates the interaction between terrain features and surface refractivity during the past decades in the North Central, Nigeria. Some issues were addressed in the study namely seasonal variation of surface refractivity over a period of 25 years (1983 – 2007), spatial distribution of surface refractivity covering 287 stations spreading across the Nigerian middle belt and relationship between terrain features and spatial variation of surface refractivity. Satellite-measured meteorological parameters comprising air temperature, relative humidity and pressure at 2 m height (relative to the surface) were obtained from National Aeronautic Space Administration (NASA) and used to compute annual, January and July averages of surface refractivity over the period. The results of surface refractivity were interpolated and compared with North Central terrain features to establish a correlation. Surface refractivity reduced with increasing altitude across the North Central, Nigeria; the reduction at interval of 100 m height was at an average of 1.27 N-Units. On the average, refractivity gradient varied at the rate of 7.87 N-Units/km. The least altitudinal variation occurred at the boundary layer while the highest variation occurred at 800 m and above. Surface refractivity and refractivity gradients at North Central, Nigeria were influenced by topographical features and the prevailing atmospheric conditions which are dependent on the seasonal rainfall regimes.

**Keywords:** Topography, Surface refractivity, propagation mode, climate, refractivity contour

**1.0 Introduction**

Radio propagation in a terrestrial environment is an enigmatic phenomenon whose properties are difficult to predict. This is particularly true at very high frequency (VHF), ultra high frequency (UHF), and super high frequency (SHF) where the clutter of hills, trees, and houses and the ever-changing atmosphere provide scattering obstacles with sizes of the same order of magnitude as the wavelength (Hagn, 1980). The engineer who is called upon to design radio equipment and radio systems does not have available any precise way of knowing what the characteristics of the propagation channel will be nor how it will affect operations. Instead, the engineer must be content with one or more models of radio propagation with techniques that attempt to describe how the physical world affects the flow of electromagnetic energy.

Line - of - sight (LOS) microwave links are prone to severe fading due to refraction of the transmitted waves along the propagation path. Hence, refractive fading can significantly impair service on terrestrial LOS microwave transmission. Microwave propagation through the troposphere is affected by varieties of natural phenomena caused by some meteorological parameters, such as pressure, temperature and relative humidity at UHF and microwave frequencies (Adeyemi and Emmanuel, 2011). These effects are analyzed from the study of radio refractive index derived from these parameters. These parameters vary considerably diurnally and seasonally in the tropics. Therefore, the

knowledge of the refractivity is essential in order to design reliable and efficient radio communication (terrestrial and satellite) systems. Thus, the refractive index of the troposphere is very important for estimating the performance of terrestrial radio links.

Profiles of refractivity gradients within 1 km of the atmosphere are important for the estimation of some propagation parameters, such as super refraction and ducting phenomena, and their effects on radar observations and VHF field strength at points beyond the horizon (Yongkang *et al.*, 2013). Multipath effects also arise due to large scale variations in atmospheric radio refractive index, such as horizontal layers with very different refractivity (Willoughby *et al.*, 2002). This effect becomes noticeable, when the same signal takes different paths to its target and the rays arriving at different times thereby interfering with each other during propagation through the troposphere. The consequence of this large scale variation in the atmospheric refractive index is that radio waves propagating through the atmosphere become progressively curved towards the earth. Thus, the range of the radio waves is determined by the height dependence of the refractivity. Therefore, the refractivity of the atmosphere will not only affect the curvature of the ray path but will also provide some insight into the fading of radio waves through the troposphere (Grabner and Kvicera, 2008).

Some of the radio refractivity models which depend on radiosonde measurements treat very specialized subjects such as micro-wave mobile data transfer in high-rise urban areas; others try to be as generally applicable as Maxwell's equations and to represent, if not all, at least most, aspects of physical reality. Although, results from radiosonde measurements lack the required resolution and coverage which is necessary for the investigations of spatial and temporal variations of surface refractivity particularly in the lower atmosphere and therefore were unable to resolve the spatial and temporal patterns emerging in the light of climate variations (Li *et al.*, 2007). Moreover, data gaps also exit while some of the stations have become defunct. In this research we shall investigate the influence of topography on surface refractivity over North Central, Nigeria using 25-year averaged satellite-based meteorological data. This is with the aim of generating refractivity and refractivity gradient contour maps for terrestrial communication planning in highly undulating characteristic nature of North Central, Nigeria.

## 2.0 Theoretical Background

Saturation vapour pressure (SVP), an important parameter in the estimation of mixing ratio, is the maximum possible vapor pressure at a given temperature. Saturation vapour pressure increases as air temperature increases. The condensation of water vapor begins after the saturation vapor pressure is reached. Therefore, SVP is given in terms of temperature as (earth science, 2015):

$$SVP = 6.11e^{\left(\frac{17.67(T-T_0)}{T-29.65}\right)} \quad 1.0$$

T is surface air temperature in Kelvin while  $T_0$  is absolute temperature equal to 273.16 Kelvin.

Mixing ratio ( $w_s$ ) is the amount of water vapor that is in the air. It is the grams of vapor per kg of dry air.  $w_s$  is an absolute measure of the amount of water vapor in the air. It can be expressed in terms of SVP and air pressure as:

$$w_s = 0.622 \times \frac{SVP}{P} \quad 2.0$$

$w_s$  is the boundary layer mixing ratio (dimensionless) and  $P$  is surface air pressure

Relative humidity can therefore be expressed as the ratio of water vapor mixing ratio to saturation water vapor mixing ratio. It is given as (Bean *et al.*, 1966):

$$RH = \frac{100 \times Q}{w_s} \quad 3.0$$

where  $Q$  is specific humidity

The relationship between water vapour pressure  $e$  and relative humidity (RH) is given by

$$e = \frac{RH \times SVP}{100} \text{ (hPa)} \quad 4.0$$

The dry term,  $N_{dry}$  of radio refractivity is given by

$$N_{dry} = 77.6 \frac{P}{T} \quad 5.0$$

The wet term,  $N_{wet}$  of radio refractivity Index is given by

$$N_{wet} = 3.732 \times 10^5 \frac{e}{T^2} \quad 6.0$$

The radio refractivity of air for frequencies up to 30 MHz is given by (ITU-R, 2003)

$$N = 77.6 \frac{P}{T} + 3.73 \times 10^5 \frac{e}{T^2} \quad 7.0$$

where  $P$  is the total atmospheric pressure in millibars (mb),  $T$  is the absolute temperature in degrees Kelvin (K), and  $e$  is the partial pressure of water vapour in millibars.

The surface refractivity parameter referenced to sea level which is necessary to calculate refractivity at any altitude,  $z$ , in kilometers, ( $N_z$ ) is given by tropospheric equation (Bean *et al.*, 1966):

$$N_z = N_{dry} \times e^{\left(-\frac{z}{H_D}\right)} + N_{wet} \times e^{\left(-\frac{z}{H_W}\right)} \quad 8.0$$

$H_D$  and  $H_W$  are dry term and wet term tropospheric scale height (in kilometers) respectively;  $Z$  is the altitude above the sea level. The equation is valid for  $Z < Z_t$  where  $Z_t$  is the mean density tropopause altitude in km. it is dependent on seasonal changes in a climatic zone (Bean *et al.*, 1966).

### 3.0 Methodology

#### 3.1 Study Area

North Central, Nigeria comprises of six administrative states namely Benue, Kogi, Kwara, Nassarawa, Niger, Plateau and Federal Capital Territory, Abuja spreading over 269,147 square kilometers with a population of over 27 million people. The geopolitical zone is situated between latitude  $7^0N$  and  $11^0N$ ; it has climatic characteristic of tropical rain forest towards the southern part and

Guinea savannah towards the northern part. Some significant remote sensing ground receiving stations belonging to National Centre for Remote Sensing, Jos; National Space Research and Development Agency, Abuja, etc. are domiciled in the zone. The zone has uniqueness of highly undulating terrain ranging between 26 m at Lokoja in Kogi State and 1205 m at Jos in Plateau State. The zone has prevalence of Guinea savannah climate; rainfall is not uniformly distributed, location beyond 13°N have monomodal regime while locations below 10°N have bimodal regime (Hayward and Oguntuyinbo, 1987). The rainy period on the average comprises of 7 months (April – October) and it ranges between 500 mm and 1, 500 mm per year. Temperature varies in the zone with daily average maximum of 32°C except in Jos where temperature ranges between 18°C and 22°C. The map of the study area is shown in figure 1.

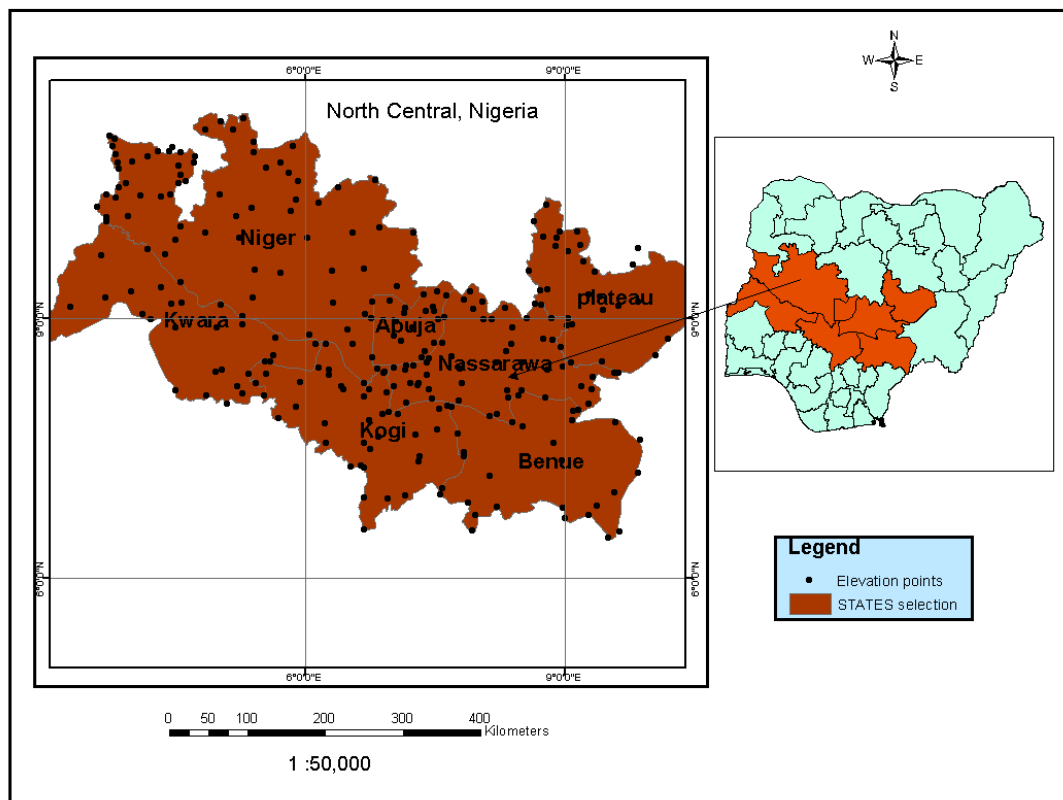


Figure 1: Thematic Map of North Central, Nigeria

### 3.2 Data Structure

National Aeronautics and Space Administration (NASA) through its' Earth science research program has long supported satellite systems and research providing data important to the study of climate and climate processes (Yongkang *et al.*, 2013). These data include long-term estimates of meteorological quantities and surface solar energy fluxes. These satellite and modeled based products have also been shown to be accurate enough to provide reliable solar and meteorological resource data over regions where surface measurements are sparse or nonexistent, and offer two

unique features – the data is global and, in general, contiguous in time (Briggs *et al.*, 2003). The dataset used in this study were extracted from Goddard Earth Observing System Model, version 5, (GEOS-5) covering the area between 3.75°N to 20.93°N and 1.16°E to 17.50°W, from 1983 through 2007 with resolution and 3-hourly output, and currently represent the best consistent estimate of the land surface processes over West Africa (Okamoto and Derber, 2006).

Satellite meteorological point data from Goddard Earth Observing Satellite Model, version 5, (GEOS-5) comprising air temperature, specific humidity and atmospheric pressure averaged monthly within 2 m height for a period of 25 years 1983 – 2007 were obtained from NASA databank as shown in Table A.1 (see Appendix 1 for sample data). Elevation values for 287 locations across North Central, Nigeria were randomly picked from Google Earth Satellite image. Also, a shape file showing the map of the study area was also obtained.

### **3.3 Data Analysis and Map Generation**

Annual mean values of the meteorological parameters were obtained by averaging the monthly recorded data. Relative humidity was calculated from specific humidity using equations 1.0 – 3.0. Dry term and wet term of surface refractivity were estimated using equations 5.0 and 6.0 respectively. Surface refractivity was obtained from the results of dry and wet terms using equation 7.0.  $H_D$  and  $H_W$  are dry term and wet term tropospheric scale height (in kilometers); they are latitudinal and seasonal dependent, the values for the months of January and July were obtained from Bean *et al.*, (1966) to calculate  $N_z$  values at a referenced height of 2 km across North Central, Nigeria. Gradients of surface refractivity were estimated within a height of 2 km above the sea level.

Elevation values comprising 287 point values were interpolated and rasterized using Geographic Information System (GIS) with a view to generate 2-dimensional elevation model. The overall mean values of surface refractivity for a period of 1983 – 2007 for 287 gridded points were obtained by averaging the monthly data, which were in turn averaged to get the mean annual values of the data. Microsoft EXCEL was used to carry out all the calculations. Surface refractivity contours were prepared and overlaid on the elevation model map to deduce its correlation with elevation patterns across the study area. The flowchart showing the procedure for data analysis is shown in Figure A.1 in the Appendix. Gradients of surface refractivity for the months of January and July were interpolated and rasterized to generate propagation characteristic map over North Central, Nigeria.

### **4.0 Spatial Patterns of Surface Refractivity over North Central, Nigeria**

Figures 2, 3 and 4 showed the maps of surface refractivity contours averaged for annual, January and July respectively. The averaged values covered a period of 1983 – 2007. The refractivity contours were overlaid on elevation model represented by graduating colours in 10 classes showing highly undulating feature of topography at North Central, Nigeria. The contour lines were generated from surface refractivity calculated for 287 geographic points by Geographic Information System (GIS) software while the elevation values (z values) were interpolated and rasterised to determine elevation model at North Central, Nigeria.

Figure 2 compared elevation model with annual average of surface refractivity (1983 – 2007). It was observed that surface refractivity reduced with increasing altitude. Reduction in surface refractivity at intervals of 100 m altitude was at an average of 1.26 N-Units at North Central, Nigeria. Altitude within 0 – 99 m had average surface refractivity of 267.32 N-Units; 100 – 199 m had 265.47 N-Units; 200 – 299 m had 264.57 N-Units; 300 – 399 m had 262.69 N-units; 400 – 499 m had 261.11 N-Units; 500 – 599 m had 260.57 N-Units; 600 – 699 m had 259.65 N-Units; 700 – 799 m had 255.72 N-Units; 800 – 899 m had 255.44 N-Units; 900 – 999 m had 254.27 N-Units; 1000 – 1099 m had 253.52 N-Units and 1100 – 1200 had 253.44 N-Units.

In figure 3, averaged value of surface refractivity in January (1983 – 2007) was compared with altitude features. The values of surface refractivity in January were typical of the peak of dry season (Harmattan) when the dry dust-laden north-easterly air mass is prevalent over the North Central, Nigeria.

Surface refractivity also reduced with increasing altitude across the North Central, Nigeria; the reduction at interval of 100 m was at an average of 1.27 N-Units. Altitude within 0 – 99 m had average surface refractivity of 258.70 N-Units; 100 – 199 m had 256.30 N-Units; 200 – 299 m had 255.47 N-Units; 300 – 399 m had 253.68 N-units; 400 – 499 m had 251.99 N-Units; 500 – 599 m had 251.46 N-Units; 600 – 699 m had 250.26 N-Units; 700 – 799 m had 246.93 N-Units; 800 – 899 m had 246.62 N-Units; 900 – 999 m had 245.50 N-Units; 1000 – 1099 m had 245.27 N-Units and 1100 – 1200 had 244.74 N-Units. The highest altitudinal variations were observed at 0 – 99 m (2.53 N-units) and 600 – 699 m (3.92 N-Units). Lowest altitudinal variations were observed at 900 – 999 m (0.23 N-Units) and 700 – 799 m (0.31 N-Units).

In figure 4, the values of surface refractivity were typical of the peak of rainy season when the warm, moist south-westerly air mass is prevalent over the entire North Central, Nigeria. Surface refractivity reduced in altitude intervals of 100 m at 1.11 N-Units. Surface refractivity variation with respect to topographic altitude in July was not as high as that of January because the surface was more saturated with moisture in the rainy season thereby making water vapour in the air to be relatively high and stable.

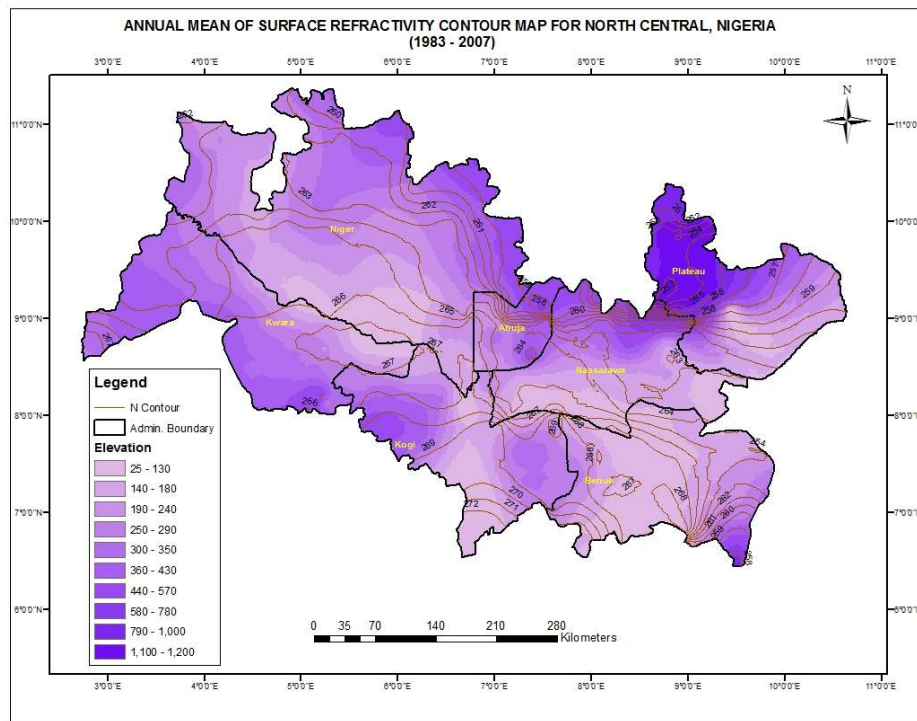


Figure 2: Spatial Patterns of Annual Surface Refractivity with Elevation (1983-2007) at North Central, Nigeria

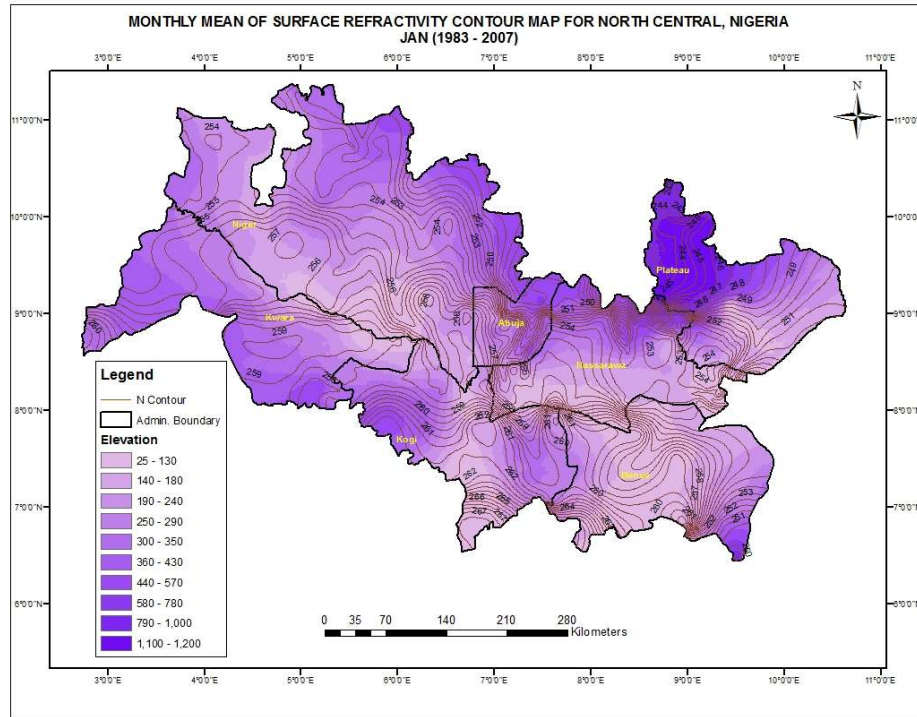


Figure 3: Spatial Patterns of Surface Refractivity with Elevation in January (1983-2007) at North Central, Nigeria

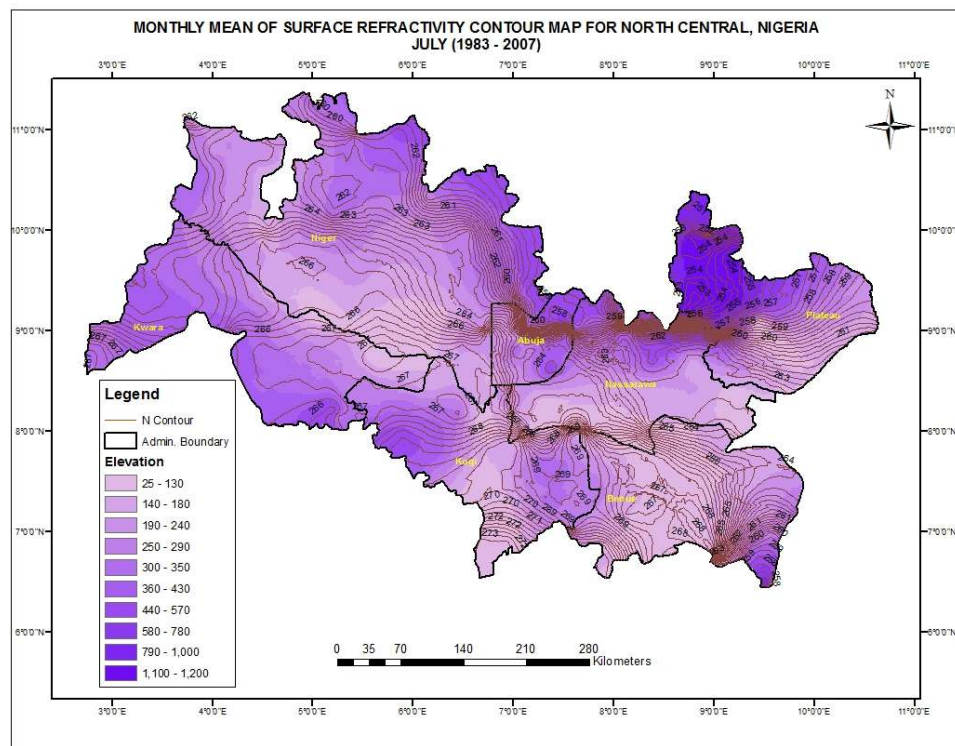


Figure 4: Spatial Patterns of Surface Refractivity with Elevation in July (1983-2007) at North Central, Nigeria

Altitude within 0 – 99 m had average surface refractivity of 271.54 N-Units; 100 – 199 m had 270.01 N-Units; 200 – 299 m had 269.33 N-Units; 300 – 399 m had 268.26 N-units; 400 – 499 m had 266.62 N-Units; 500 – 599 m had 266.19 N-Units; 600 – 699 m had 265.15 N-Units; 700 – 799 m had 261.98 N-Units; 800 – 899 m had 260.87 N-Units; 900 – 999 m had 260.21 N-Units; 1000 – 1099 m had 230.41 N-Units and 1100 – 1200 had 259.28 N-Units. The highest altitudinal variation was observed at 600 – 699 m (3.16 N-Units) while the lowest altitudinal variation was at 400 – 499 m (0.42 N-Units).

## **5.0 Surface Refractivity Gradient Patterns over North Central, Nigeria**

Figures 5, 6, and 7 showed the maps of surface refractivity gradient classified into different propagation characteristics such as sub-refraction, normal refraction, super-refraction and ducting. Twenty-five years results from 287 stations were selected for use in the preparation of these maps because large number of stations is desirable for mapping purposes (better coverage), while longer periods of record yield more stable (accurate) estimates of long-term means (of climatic variables).

Specific information on the gradient of the surface refractivity, most especially at North Central, Nigeria, has not been available previously on such a large scale basis, especially for the very important layers of the atmosphere at or near the surface where the presence of super-refractive or ducting gradients can produce anomalous propagation of microwaves. The values in figures 5, 6 and 7 were refractivity gradients at altitude 2 km and referenced to sea-level over the area. It was observed that the propagation mode at a desired altitude was influenced by topographic features in the boundary layer.

In figure 5, it was observed that altitude within 0 – 99 m had sub-refractivity propagation mode; 100 – 199 m had normal refractivity propagation; 200 – 999 m had super-refractivity mode while ducting was observed at altitude beyond 1000 m at North Central, Nigeria. In general, surface refractivity gradient was influenced by topographic features. On the average, refractivity gradient varied at the rate of 7.87 N-Units/km. The least altitudinal variation occurred at the boundary layer while the highest variation occurred at 800 m and above.

Figure 6 showed the averaged surface refractivity gradient patterns in January (1983 – 2007). It was observed that altitude within 0 – 299 m had prevalence of sub-refractivity propagation mode; 300 – 1099 m had super-refractivity propagation while ducting was observed at altitude beyond 1100 m. On the average, refractivity gradient varied at the rate of 6.86 N-Units/km. The least altitudinal variation occurred at the boundary layer while the highest variation occurred at altitude beyond 800 m.

Figure 7 showed the averaged surface refractivity gradient patterns in July (1983 – 2007). It was observed that altitude within 0 – 99 m had prevalence of sub-refractivity propagation mode; 100 – 1099 m had super-refractivity propagation while ducting was observed at altitude beyond 1100 m. On the average, refractivity gradient varied at the rate of 8.47 N-Units/km. The least altitudinal variation occurred at altitude within 900 - 999 while the highest variation occurred at altitude beyond 1100 m.

## **6.0 Conclusion**

Surface refractivity and refractivity gradients at North Central, Nigeria were influenced by topographical features and the prevailing atmospheric conditions which are dependent on the seasonal rainfall regimes. The dry Harmattan season has been found to favour sub-refraction at lower altitude but significantly reduced in the rainy month of July thereby leading to prevalence of super-refraction propagation mode. It is not only the evaporation gradient and surface moisture that highly correlated with surface radio refractivity, but a combination of vegetation properties and topography. Therefore, it is the very particular combination of moisture gradients, vegetation distribution and topography that produces spatial variability of surface refractivity and refractivity gradients patterns.

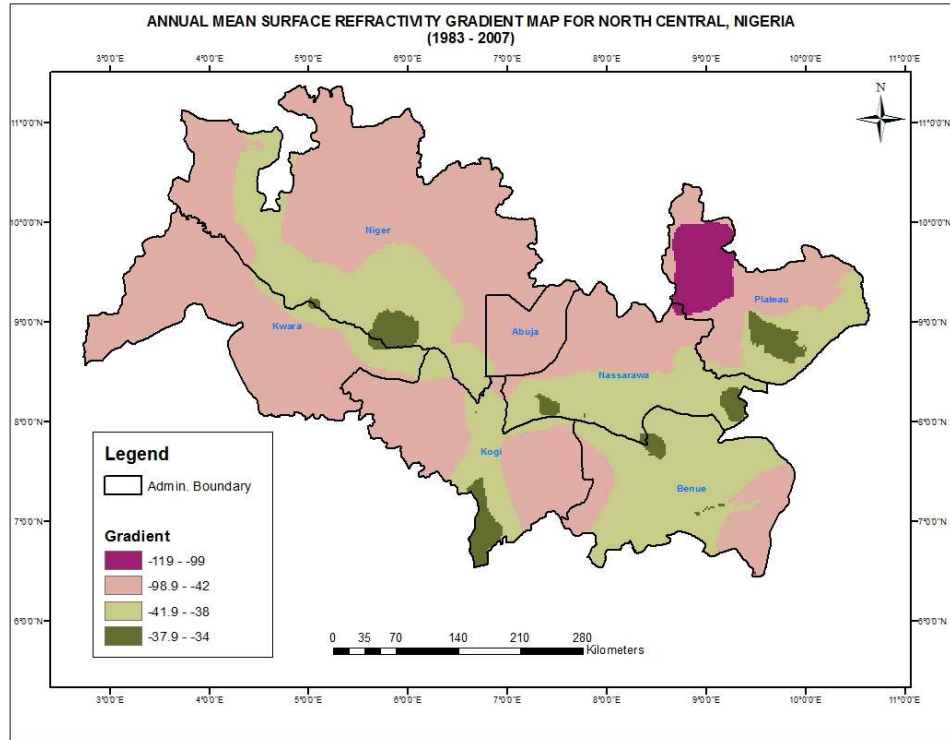


Figure 5: Annual Mean of Refractivity Gradient Patterns (1983-2007) at North Central, Nigeria

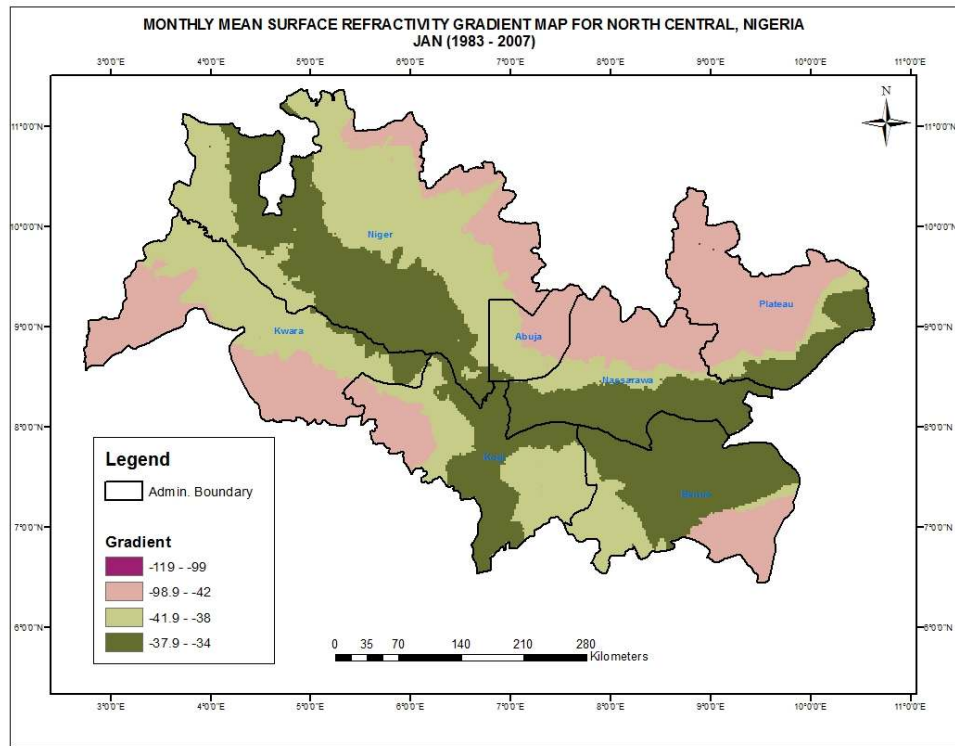


Figure 6: Monthly Mean of Refractivity Gradient Patterns in January (1983-2007) at North Central, Nigeria

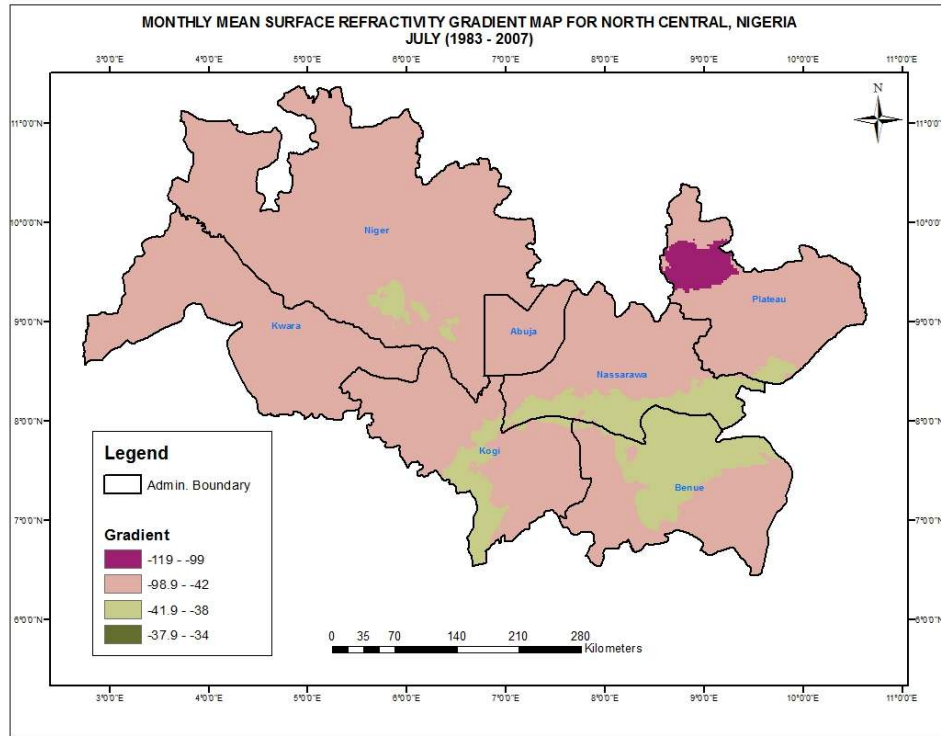


Figure 7: Monthly Mean of Refractivity Gradient Patterns in July (1983-2007) at North Central, Nigeria

## 7.0 Acknowledgement

The authors wish to appreciate National Aeronautics and Space Administration (NASA) and en.tutiempo.net for their long supported satellite systems and research providing data important to the study of climate and climate processes. Archived meteorological were made available through the online databank services for the research.

## 8.0 REFERENCES

1. Adeyemi, B and Emmanuel, I (2011): Monitoring tropospheric radio refractivity over Nigeria using CM – SAF data derived from NOAA – 15, 16 and 18 satellites. Indian Journal of Radio and Space Physics, (40) pp. 301 – 310.
2. Bean, B. R., Cahoon, B. A., Samson, C. A and Thayer, G. D (1966): **A World Atlas of Atmospheric Radio Refractivity**, Institute for Telecommunication Sciences and Aeronomy, Boulder, Colombia, pp. 29
3. Briggs, S., Lucas, R. G. and Taylor, Z. T. (2003): Climate Classification for Building Energy Codes and Standards. Technical Paper, Pacific NW National Laboratory, March 26
4. <http://earthscience.stackexchange.com/questions/2360/how-do-i-convert-specific-humidity-to-relative-humidity> (2015)
5. Dai, A., Lamb, P., Trenberth, K. E., Hulme, M., Jines, P. D., and Xie, E. (2004): "The recent Sahel drought is real" International Journal of Climatology. Vol. 24, pp. 1323-1331

6. Grabner, M. and Kvicera, V. (2008): Radio Engineering Vol. 12, No.4, pp. 50
7. Hagn, G. H. (1980): VHF radio system performance model for predicting communications operational ranges in irregular terrain, IEEE Trans. Commun. COM-28, pp. 1637-1644.
8. Hayward and Oguntuyinbo J. S. (1987): Variability of the Precipitation (1951 – 1960) in Respect of the Long-Term Mean Annual Precipitation for Some Selected Stations in West Africa, pp. 25 - 30
9. ITU-R, (2003): “Radio Refractive Index: Its Formula and Refractivity Data”, International Telecommunication Union Radio-communication, Geneva, pp. 453-459
10. Li, W. P., Xue, Y. and Pocard, I. (2007): “Numerical investigation of the impact of vegetation indices on the variability of West African summer monsoon”, Journal of Meteorological Society of Japan, Vol. 85A, pp. 363-383
11. Okamoto, K. and Derber, J. (2006): Assimilation of Radiances in the National Centres for Environmental Prediction (NCEP) Global Data Assimilation System. Monthly Weather Review, Vol. 134, pp. 2612-2631
12. Philippon, N., Jarlan, L., Martiny, N. and Camberlin, P. (2007): “Characterization of the Inter-annual and Intra-seasonal Variability of West African Vegetation between 1982 and 2002 by Means of NOAA AVHRR NDVI Data”. Journal of Climate, Vol. 20, pp. 1202-1218
13. United Nations Office for West Africa: West Africa, <http://unowa.unmissions.org/Default.aspx?tabid=793>.
14. Willoughby, A., Aro, T. O. and Owolabi, I. E. (2002): Journal of Atmospheric Science and Solar-Terrestrial Physics, Vol. 64, pp. 417
15. Yongkang X., Aaron B., and Christopher M. T. (2013): Review of Recent Developments and the Future Prospective in West African Atmosphere/Land Interaction Studies. Department of Atmospheric & Oceanic Sciences University of California, Los Angeles, CA 90095, USA pp. 1 – 4

## APPENDIX

Table A.1: Sample of Surface Meteorological Data obtained from NASA Databank

States	Latitude	Longitude	Elevation (m)	Pressure (hPa)	Temp (Deg C)	Specific Humidity
Niger	11.10	3.74	248	981.6	28.01	0.012120
Niger	10.80	4.00	228	980.1	26.83	0.013333
Niger	10.42	3.70	345	978.6	26.94	0.013165
Niger	9.73	4.38	224	980.7	26.21	0.014400
Kwara	8.84	2.87	326	982.2	25.63	0.015454
Kwara	9.13	3.29	401	976.5	25.95	0.014329
Kwara	8.89	4.98	239	979.9	25.44	0.015394
Kwara	9.15	5.03	84	981.7	26.29	0.014370
Kogi	8.26	5.94	320	981.8	25.71	0.015213
Kogi	8.34	6.28	236	981.7	25.78	0.014986
Kogi	7.65	7.28	350	986.2	25.53	0.015530
Kogi	7.63	6.85	134	986.4	25.52	0.015758
Abuja	9.19	6.77	251	974.7	25.86	0.014136
Abuja	8.99	6.76	186	981.7	25.78	0.014986
Abuja	8.89	7.24	312	974.2	25.27	0.014587
Abuja	9.08	7.39	474	956.6	24.75	0.013537
Nassarawa	7.79	8.40	79	982.7	26.36	0.015180
Nassarawa	8.08	8.35	124	968.7	25.08	0.014124
Nassarawa	9.00	9.04	855	954.2	24.96	0.012687
Nassarawa	8.91	9.03	587	970.5	25.31	0.013810
Benue	6.72	7.97	133	990.3	25.28	0.016302
Benue	6.82	8.22	114	979.8	24.77	0.015817
Benue	6.44	9.67	391	950.4	23.71	0.014705
Benue	6.37	9.54	333	950.4	23.71	0.014705
Plateau	9.48	10.54	214	963.2	25.67	0.012625
Plateau	8.91	10.63	135	967.1	25.41	0.013420

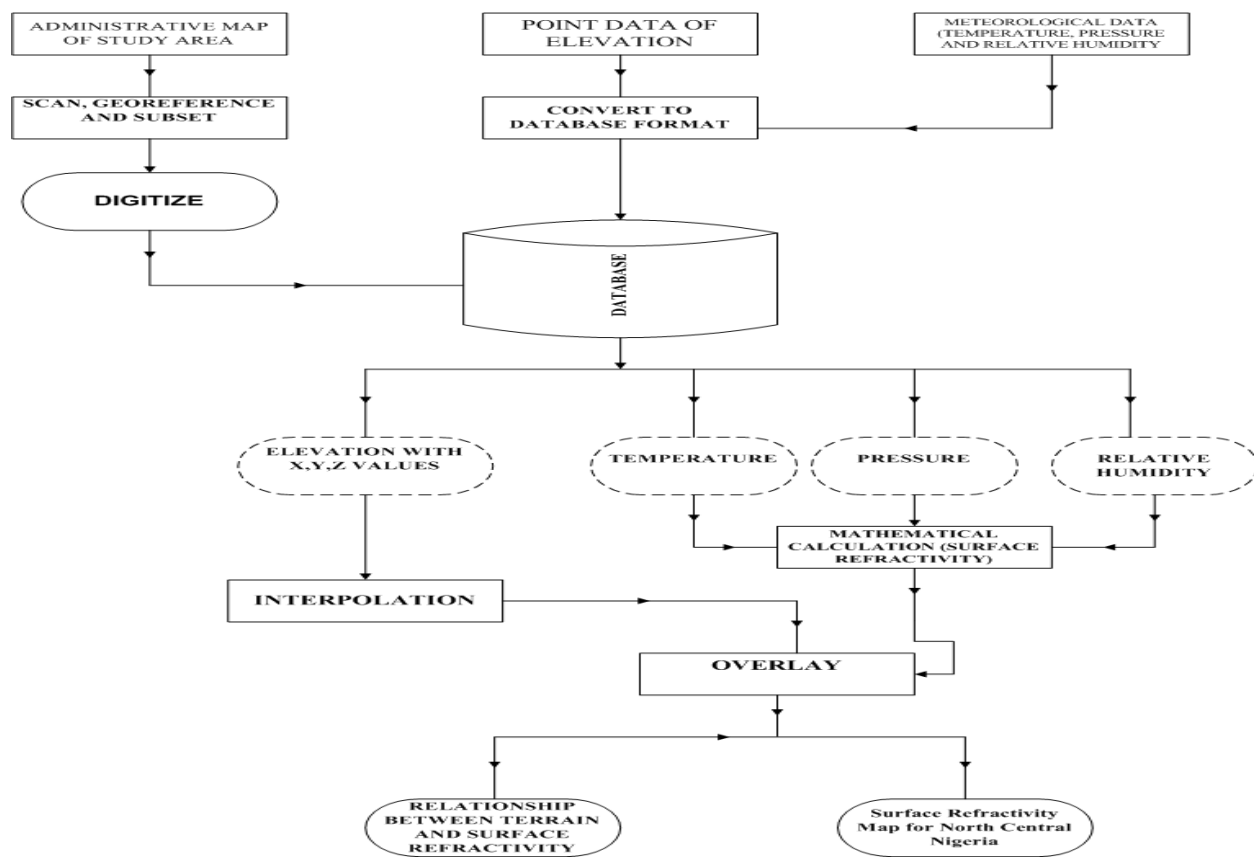


Figure A.1: Research Workflow showing Data Procedure Analysis